

15. 2020,M. Taufiqurrahman, Moh.  
Toifur, Ishafit, Okimustafa, Azmi  
Khusnani.pdf

2

International Journal of Advanced Research in Engineering and Technology (IJARET)

1 Volume 11, Issue 10, October 2020, pp. 333-341, Article ID: IJARET\_11\_10\_035

Available online at <http://www.iaeme.com/IJARET/issues.asp?JType=IJARET&VType=11&IType=10>

ISSN Print: 0976-6480 and ISSN Online: 0976-6499

DOI: 10.34218/IJARET.11.10.2020.035

© IAEME Publication



Scopus Indexed

# EFFECT OF SOLUTION TEMPERATURE ON VOLTAGE RANGE AND SENSITIVITY OF LOW-TEMPERATURE SENSOR CU/NI RESULTS FROM ELECTROPLATING ASSISTED BY PARALLEL MAGNETIC FIELDS

M. Taufiqurrahman, Moh. Toifur\*, Ishafit, Okimustafa, Azmi Khusnani

3 Magister of Physics of Physic Education,  
Faculty of Teacher Training and Education,  
The Ahmad Dahlan University, Indonesia

## ABSTRACT

This study aims to identify the effect of solution temperature aided by parallel magnetic fields on the sensitivity and voltage range of the Cu/Ni sensor as a low-temperature sensor. Solution temperature was varied from 30°C-70°C. The results of data analysis showed that the highest sensitivity is a sensor which is deposited at a temperature of 60°C with a sensitivity level  $(0.118 \pm 0.004) \text{ mV/}^\circ\text{C}$  with  $R^2 = 0.98$  and sensor which has the lowest sensitivity sensor with the deposition temperature of 30°C is  $(0.0004 \pm 0.007) \text{ mV/}^\circ\text{C}$  with  $R^2 = 0.96$ . In contrast to the sensitivity, the highest voltage range is 39.67 mV owned by the sensor which is deposited at 30°C and 60°C while the lowest voltage range is 32.04 mV as a result of the deposition temperature of 40°C.

**Key words:** Sensitivity, voltage range, thin film Cu/Ni, electroplating, parallel magnetic field

**Cite this Article:** M. Taufiqurrahman, Moh. Toifur, Ishafit, Okimustafa and Azmi Khusnani, Effect of Solution Temperature on Voltage Range and Sensitivity of Low-Temperature Sensor CU/NI Results from Electroplating Assisted by Parallel Magnetic Fields, *International Journal of Advanced Research in Engineering and Technology*, 11(10), 2020, pp. 333-341.

<http://www.iaeme.com/IJARET/issues.asp?JType=IJARET&VType=11&IType=10>

## 1. INTRODUCTION

The availability of Cryogenic sensors in the 21st century has become a very important requirement. Cryogenic sensors are widely used in various fields, including in the aerospace and nuclear fields [1], livestock field [2], health sector, even in the food industry [3]. Cryogenic sensors that are quite popularly used are thermocouple and temperature detector

1

<http://www.iaeme.com/IJARET/index.asp>

333

[editor@iaeme.com](mailto:editor@iaeme.com)

(RTD) resistance sensors [4]. Cryogenic temperature is known to be very low, namely  $-196^{\circ}\text{C}$  [5]. However, in many measurement cases, errors in the thermocouple sensor often occur because they are unable to measure the assumed temperature. In contrast to the RTD sensors that have high accuracy with excellent output [6-7]. The basic working principle of the RTD sensor is to take advantage of changes in material resistance to temperature changes [8]. The resistance of the material will increase when the temperature increases, and vice versa. The change in resistance occurs which is proportional to temperature. At the beginning of its development, RTD was in the form of a wire-wound (RTD-C), but over time it began to be replaced by a resistance temperature detector film (RTD-F) [9-10]. The RTD-C sensor has the disadvantages of a low measurement range. In contrast to the RTD-F sensor which has a faster thermal response and a better sensor sensitivity level [11].

There are several materials commonly used as materials for making RTDs. Usually made of pure metal elements such as platinum (Pt) [12], Nickel (Ni) [13], and copper (Cu) [14]. However, in this study, Cu and Ni were synthesized. Basically, Cu has the potential to be a temperature sensor [15], it's just that Cu is still less sensitive to temperature changes. This is because the resistivity possessed by Cu tends to be very low [16] as well as the nature of Cu which is easily oxidized. Basically, Cu sensitivity can be increased by synthesizing it with Ni which has a higher resistivity value, namely Ni to form a thin layer structure of Cu/Ni. Another advantage of Ni is that it has a better adhesion force compared to Pt, making it easier for film deposition [17]. Cu/Ni material also has a relatively high-temperature coefficient value [18]. So it is very suitable to be applied as a low-temperature sensor. Based on these advantages, the reasons for choosing Cu and Ni in this study. The synthesis method used in this research is electroplating because it is more economical, fast, with a process that is easy to control [18]. Electroplating is carried out with temperature variations aided by parallel magnetic fields. The role of parallel magnetic fields is to form a more regular and uniform distribution of particles [19]. The use of magnetic fields also plays a role in increasing the mass deposition of articles [20]. This results in a more homogeneous Ni layer structure. Then temperature plays an important role in reducing the viscosity of the solution so as to facilitate the rate of ion deposition [21]. The combination of these two parameters has the potential to improve the crystal arrangement to become homogeneous so as to increase the sensitivity of the sensor.

Based on previous research that carried out Cu/Ni synthesis assisted by perpendicular magnetic fields, it produces a rough layer structure. So as to produce a low sensor sensitivity, namely  $V = -7 \times 10^{-7} T^2 + 0,0003 T + 0,4746$  with a determination index of 0.99 [22]. Therefore it is important to study the effect of solution temperature aided by parallel magnetic fields on the voltage range and sensitivity of the sensor.

## 2. MATERIALS & EXPERIMENTAL PROCEDURES

This research is experimental research. The flow of this research follows the procedure shown in Figure 1.

The material needed in this research is Liquid Nitrogen ( $\text{LN}_2$ ). Meanwhile, the tools used are a computer, a TCA-BTA thermocouple, transducer, wire, voltage sensor,  $\text{LN}_2$  container, 4-WCB, mini quest lab, and Cu/Ni sensors. The specifications of the Cu/Ni sensor are 7.61 cm wide, 0.5 mm thick Cu plate, the thickness of the Ni layer structure varies from (59-133)  $\mu\text{m}$  with a square wave sample shape. Low-temperature sensor testing in this study uses  $\text{LN}_2$  as a low temperature. Because the temperature of  $\text{LN}_2$  is a cryogenic temperature of  $-196^{\circ}\text{C}$  [23]. The test is carried out very carefully, by inserting the sensor slowly in order to ensure that the reading of the data is stable without missing a temperature range. The test media used

was an LNcontainer<sub>2</sub> with a volume of LN<sub>2</sub> 10 liters of. Even though it contains LN<sub>2</sub>, the temperature inside the container varies with the difference in the distance between the sensor and the medium. The bottom temperature of the LNcontainer<sub>2</sub> is lower than the temperature at the mouth of the container. Cu/Ni sensor testing is carried out simultaneously with the TCA-BTA thermocouple sensor. Cu/Ni sensor output data with thermocouples is different because Cu/Ni sensors have output data in the form of a voltage (V) instead of temperature (T). In order to avoid contributing to the output voltage from the cable due to leakage of the voltage generated by the sensor which results in measurement errors, the sensor is connected to a 4-WCB circuit (Four Wire Configuration Bridge) [24]. The Cu/Ni sensor output voltage range used in this study is in the temperature range of 20°C to -196°C. The output data of the two sensors is observed in the form of graphical visualization and tables in the Logger Pro software. The output data is analyzed for sensor sensitivity and voltage range. Analyze sensor sensitivity based on the voltage-temperature (curve V-T), while analyzing the sensor voltage range using the maximum and minimum voltage output of the sensor.

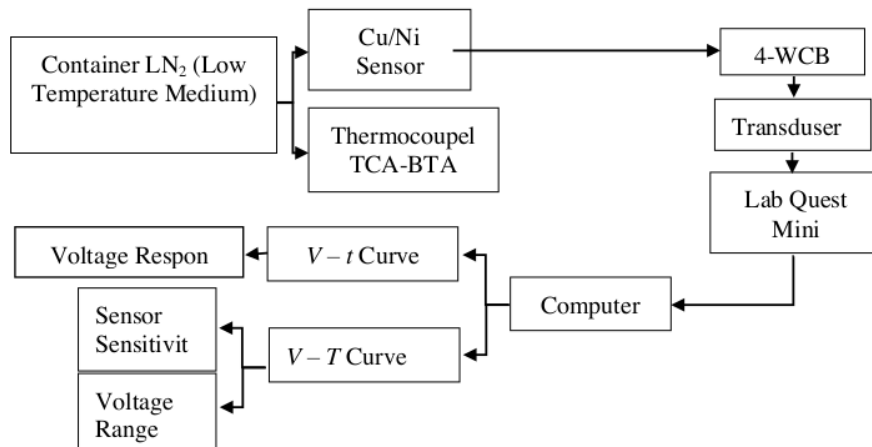


Figure 1 Research Scheme on Sensor Testing

Sensor sensitivity was analyzed using the second-order polynomial equation [25]. The most sensitive sensor is determined based on the value of *b* largest [26]. The relationship between voltage (*V*) and temperature (*T*) has a relationship which is described in the following equation [27].

$$V = aT^2 + bT + c \tag{1}$$

Where, *V* is voltage (V), *T* is temperature (°C), *a* is curvature, *b* is slope, and *c* is intercept.

### 3. RESULTS AND DISCUSSION

Figure 2 is the response of the Cu/Ni low-temperature sensor voltage to LNtemperature<sub>2</sub> in the container. The difference in output voltage response indicates that the deposition temperature of the material affects the sensor's voltage-time (*V-t*) curve. The horizontal axis of the image informs that each sensor deposited at a different solution temperature has a different response time to reach the maximum temperature of LN<sub>2</sub> [28] before returning to its original temperature. The difference in response time is caused by the microstructure of the films and the experimental parameters used in their manufacture [29]. The process of measuring sensor resistance is carried out by simultaneously inserting a thermocouple low-temperature sensor as a calibration tool. Calibration is carried out to minimize the uncertainty of data acquisition by sensors so that the resistance relationship of each sensor to temperature is obtained [30]. The RTD Cu/Ni sensor calibration process is carried out in an LNcontainer<sub>2</sub> starting at a

Effect of Solution Temperature on Voltage Range and Sensitivity of Low-Temperature Sensor  
CU/NI Results from Electroplating Assisted by Parallel Magnetic Fields

temperature of 20°C - 196°C and then maintains it for a while in the LNcontainer<sub>2</sub> until the sensor voltage decreases to its maximum state before the sensor is lifted back up again at 20°C. During the process of testing the sensor capability, the voltage-time (*V-t*) curve at a certain time appears to decrease when the temperature increases and the voltage curve rises when the temperature in the container decreases so that the voltage curve appears to be curved or offset. Such events often occur because the RTD detects the danger of thermal disturbance with high efficiency at room temperature to the initial temperature of the test [31]. The thermal disturbance in question is the difference in thermal capacitance and thermal conductivity that appears between measurement instruments. However, in general, the Cu/Ni sensor shows a linear and stable curve with thermocouple sensor output data, especially at low temperatures. The shape of the curve (*V-t*) in the sensor resistance test in this study also still has ripples in the reading of the data. This ripple is thought to arise as a result of fluctuations in the sensor that occurs for a long time due to the entry of CO<sub>2</sub> into the container, as well as the appearance of electrical disturbances that arise from the entire circuit [32]. Another cause of the presence of ripples in the sensor output voltage is due to the microstructure of the Cu/Ni sensor layer. A layer structure with a uniform and regular crystal size will produce a relatively more stable output voltage because electric current can easily flow through the layer structure. Unlike the layer structure which has non-uniform crystal size and an irregular crystal arrangement, it will inhibit the current through the layer structure so that the output voltage becomes unstable.

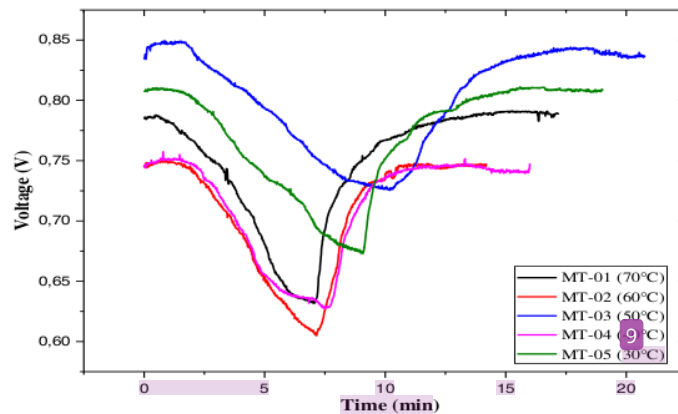
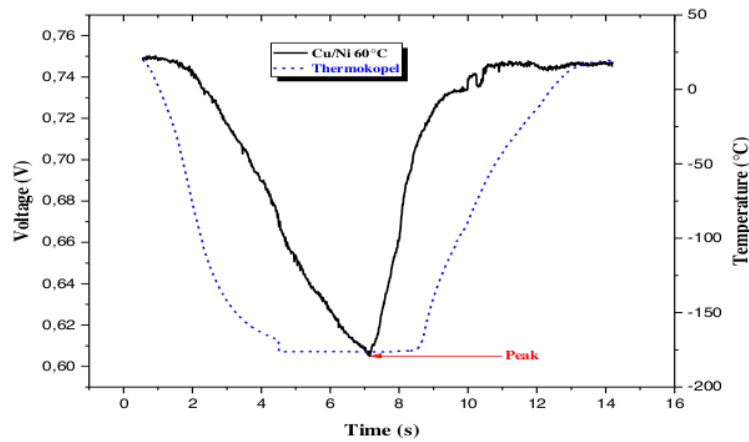


Figure 2 Cu/Ni output voltage

During the sensor resistance testing process, there is an interesting point where the resistance of the Cu/Ni sensor is much better than the thermocouple sensor. One of them is clearly visible on the RTD Cu/Ni sensor deposited at 60°C. This event occurs because the thermocouple sensor freezes so that no current flows [33]. The difference in the sensing limit of the thermocouple and Cu/Ni sensor measurements can be seen in Figure 3.



**Figure 3.** Output Voltage Cu / Ni sensor and Thermocouple Sensor

**Voltage Range.** Figure 3 is a visualization of the voltage range of each Cu/Ni sensor deposition temperature variation. The voltage range of each sensor determines the level of accuracy and precision of temperature measurements by each sensor [34].

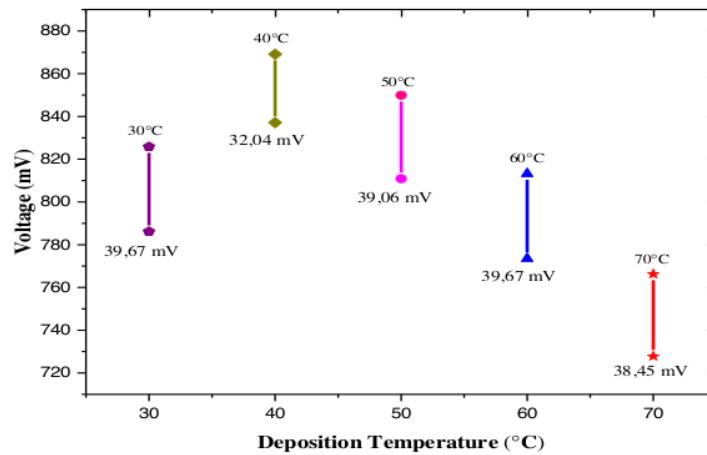


**Figure 4.** Voltage Range Sensor Cu/Ni deposited at temperature variations

Each Cu/Ni sensor output voltage range that was deposited at various temperature solutions looked different, from 32.04 mV to 39.67 mV. The highest voltage range for the Cu/Ni sensor is 39.67 mV with a deposition temperature of 30°C and 60°C. Then 38.45 mV for sensors deposited at 70°C while sensors deposited at 40°C have the smallest voltage range, namely 32.04 mV.

**Sensor Sensitivity.** The level of sensor sensitivity is determined by the accuracy of the sensor output voltage change in response to temperature changes in the LNcontainer<sub>2</sub> [27]. Data collection was set at 10 samples per second with a very slow data collection rate of 0.2 cm/s. The sensor is lowered slowly into the LNcontainer<sub>2</sub> in order to avoid gradient effects [28]. The overall output voltage of the Cu/Ni sensor tends to form a polynomial. The sensor output voltage displayed on the curve ( $V-T$ ) is a temperature range of -170°C to 0°C. The range of -170°C was chosen because it conforms to the accurate measuring limit of the thermocouple.

Effect of Solution Temperature on Voltage Range and Sensitivity of Low-Temperature Sensor  
 CU/Ni Results from Electroplating Assisted by Parallel Magnetic Fields

The relationship of voltage to temperature and the sensitivity level of the Cu/Ni sensor can be seen in Figure 5.

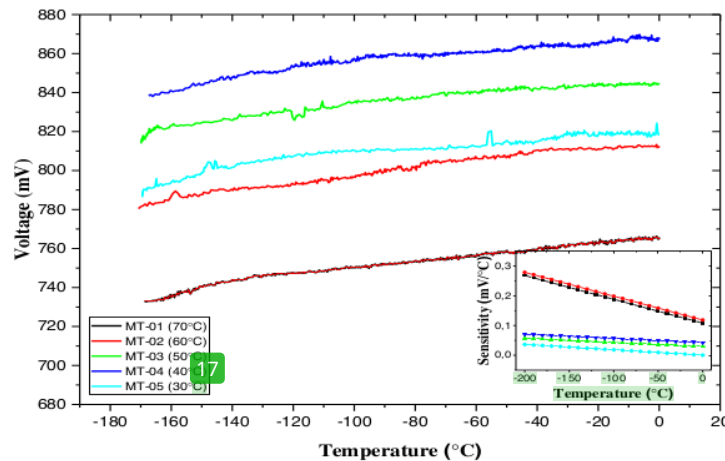


**Figure 5** Cu/Ni Sensor Voltage Responds to LN<sub>2</sub> Temperature

Based on the test results, the entire sample shows a strong tendency to decrease stress following linear regression to temperature [35]. This relationship that tends to be linear is caused by the scattering of electrons by lattice vibrations (phonons) because at high temperatures the phonons will vibrate with higher amplitude than <sup>19</sup> low temperatures [36]. This data distribution pattern is a simple form that describes the relationship between temperature and resistance in RTDs. The results of fitting Cu/Ni sensor output voltage data to LNtemperature<sub>2</sub> can be seen in Table 1.

**Table 1** Output Fitting Output Sensor Cu/Ni Sensor

Deposition Temperature (°C)	$V = aT^2 + b$	$S_b$	$R^2$
70	$-0,0004 T^2 + 0,108$	0,003	0,99
60	$-0,0004 T^2 + 0,118$	0,004	0,98
50	$-0,0007 T^2 + 0,029$	0,003	0,99
40	$-0,0007 T^2 + 0,042$	0,003	0,97
30	$-0,0009 T^2 + 0,0004$	0,007	0,96

Based on Table 2, it informs that the results fitting of the regression data ( $V-T$ ) with  $a$  and  $b$ . The entire sample shows different levels of sensitivity and data stability when tested to measure the temperature of LN<sub>2</sub> as a low-temperature sensor. However, based on the results of overall observations, it can be seen that Cu/Ni sensors deposited using high temperature are more sensitive than those using room temperature. The highest sensor sensitivity is owned by Cu/Ni sensors that are deposited with a temperature of 60°C, namely  $(0.118 \pm 0.004)$  mV/°C, and the lowest sensitivity is owned by Cu/Ni sensors that are deposited at 30°C with a sensitivity level  $(0,0004 \pm 0,007)$  mV/°C. While the stability of the sensor output data are best owned by a sensor Cu/Ni was deposited at 50°C and 70°C with an index value of determination  $R^2 = 0.99$ . While the sensor with the lowest data stability owned by sensors Cu/Ni was deposited at 30°C with an index value of determination  $R^2 = 0.96$ . Apart from seeing the value  $b$  biggest, determining the sensitivity level of the Cu/Ni sensor can also be seen from the slope of the curve shape as shown in Figure 5 because the sensor sensitivity is obtained from the slope of the resistance measurement curve to temperature [37]. So that the

tilted the resulting curve shows the higher the sensitivity level of the sensor. The high sensitivity of the test is also associated with the lack of defects in the layer structure and sufficient thickness, so it is very good at reducing electron scattering [38-39].

#### 4. CONCLUSIONS

Cu/Ni sensors with wave square lithography are made using the electroplating method at various temperature solutions with the help of parallel magnetic fields. The results showed sensor Cu/Ni was deposited at a 60°C sensor is the most sensitive and most stable solution ( $0.118 \pm 0.004$ ) mV/°C with  $R^2 = 0.98$ . Meanwhile, the highest Cu/Ni sensor voltage range is 39.67 mV with a deposition temperature of 30°C and 60°C, and the smallest voltage range is 32.04 mV as a result of deposition at 40°C. As a result, the Cu/Ni sensor that is deposited at 60°C with the RTD-F type can be a reference as a low-temperature sensor in various fields because it is very sensitive to reach temperatures of -196°C and has the highest voltage range.

#### ACKNOWLEDGMENT

“The researcher expresses his deepest gratitude to the Ministry of Research and Technology/ National Research and Innovation Agency which has provided research funding through the 20/2019 through Post Graduate Research Grant Scheme with a contract number of NOMOR: PTM-031/SKPP.TT/LPPM UAD/VI/2020”

#### REFERENCES

- [1] S. D. Jiang, J. Q. Liu, B. Yang, H. Y. Zhu, and C. S. Yang, “Microfabrication of thin film temperature sensor for cryogenic measurement,” *Microsyst. Technol.*, vol. 20, no. 3, pp. 451–456, 2014.
- [2] V. de Miguel-Soto, D. Leandro, A. Lopez-Aldaba, J. J. Beto-Lopez, J. I. Perez-Landazabal, J. L. Aguste, R. Jamier, P. Roy, and M. Lopez-Amo, “Study of optical fiber sensors for cryogenic temperature measurements,” *Sensors (Switzerland)*, vol. 17, no. 12, pp. 1–12, 2017.
- [3] S. Balasubramanian, M. J. Gupta, and K. K. Singh, “Cryogenics and its application with reference to spice grinding: a review.,” *Crit. Rev. Food Sci. Nutr.*, vol. 52, no. 9, pp. 781–794, 2012.
- [4] M. Lebioda and J. Rymaszewski, “Dynamic properties of cryogenic temperature sensors,” *Prz. Elektrotechniczny*, vol. 1, no. 2, pp. 227–229, 2015.
- [5] H. B. Shim, S. H. Nahm, I. S. Cho, and C. M. Suh, “Ultrasonic fatigue test at cryogenic temperatures on SUS304L by cold rolling ratio for LNG carriers,” *Eng. Fail. Anal.*, vol. 112, no. March, p. 104515, 2020.
- [6] W. T. Sung, J. H. Chen, and C. L. Hsiao, “Data fusion for PT100 temperature sensing system heating control model,” *Meas. J. Int. Meas. Confed.*, vol. 52, no. 1, pp. 94–101, 2014.
- [7] M. ling Zhu, “A thermometer based on diverse types thermocouples and resistance temperature detectors,” *J. Shanghai Jiaotong Univ.*, vol. 20, no. 1, pp. 93–100, 2015.
- [8] M. Simcik, M. C. Ruzicka, A. Mota, and J. A. Teixeira, “Chemical Engineering Research and Design Smart RTD for multiphase flow systems,” *Chem. Eng. Res. Des.*, vol. 90, no. 11, pp. 1739–1749, 2012.
- [9] J. Kim, J. Kim, Y. Shin, and Y. Yoon, “A Study on the Fabrication of an RTD (Resistance Temperature Detector) by Using Pt Thin Film,” *Korean J. Chem. Eng.*, vol. 18, no. 1, pp. 61–66, 2001.
- [10] Y. Wang, C. Zhang, J. Li, G. Ding, and L. Duan, “Fabrication and characterization of ITO thin film resistance temperature detector,” *Vacuum*, vol. 140, pp. 121–125, 2017.



Effect of Solution Temperature on Voltage Range and Sensitivity of Low-Temperature Sensor  
CU/NI Results from Electroplating Assisted by Parallel Magnetic Fields

- [11] J. Cui, H. Liu, X. Li, S. Jiang, B. Zhang, Y. Song, and W. Zhang, "Fabrication and characterization of nickel thin film as resistance temperature detector," *Vacuum*, vol. 176, p. 109288, 2020.
- [12] N. Miyakawa and W. Legner, "MEMS-based microthruster with integrated platinum thin film resistance temperature detector ( RTD ), heater meander and thermal insulation for operation up to 1 , 000 ° C," *Microsyst Technol*, vol. 18, pp. 1077–1087, 2012.
- [13] Q. Li, L. N. Zhang, X. M. Tao, and X. Ding, "Review of Flexible Temperature Sensing Networks for Wearable Physiological Monitoring," *Adv. Healthc. Mater.*, vol. 6, no. 12, pp. 1–23, 2017.
- [14] T. Yang, D. Xie, Z. Li, and H. Zhu, "Recent advances in wearable tactile sensors: Materials, sensing mechanisms, and device performance," *Mater. Sci. Eng. R Reports*, vol. 115, pp. 1–37, 2017.
- [15] E. K. Athanassiou, R. N. Grass, and W. J. Stark, "Large-scale production of carbon-coated copper nanoparticles for sensor applications," *Nanotechnology*, vol. 17, no. 6, pp. 1668–1673, 2006.
- [16] A. N. S. Bin Awangku Metosen, S. C. Pang, and S. F. Chin, "Nanostructured multilayer composite films of manganese dioxide/nickel/copper sulfide deposited on polyethylene terephthalate supporting substrate," *J. Nanomater.*, vol. 2015, no. April, 2015.
- [17] A. Garraud, P. Combette, and A. Giani, "Thermal stability of Pt/Cr and Pt/Cr2O3 thin-film layers on a SiNx/Si substrate for thermal sensor applications," *Thin Solid Films*, vol. 540, pp. 256–260, 2013.
- [18] S. Prasad, Dora, S. Ebenezer, Nitla, C. Shoba, and S. Rao, Pujari, "Effect of nickel electroplating on the mechanical damping and storage modulus of metal matrix composites," *Mater. Res. Express*, 2018.
- [19] L. Aguilera, Y. Leyet, Y. Romaguere-Barcelay, E. H. N. S. Thaines, A. J. Terezo, G. L.C. Souza, R. G. Frietas, R. R. Passos, and L.A. Pocrifka, "Influence of electrodeposition temperature in the electrochemical properties of Ni(OH)2: An experimental and theoretical study," *Thin Solid Films*, vol. 670, pp. 24–33, 2019.
- [20] A. Krause, M. Uhlemann, A. Gebert, and L. Schultz, "The effect of magnetic fields on the electrodeposition of cobalt," *Electrochim. Acta*, vol. 49, no. 24, pp. 4127–4134, 2015.
- [21] J. Wustha, M. Toifur, A. Khusnani, and O. Mustava, "Microstructure and resistivity of Cu/Ni thin film prepared by magnetized electroplating on various electrolyte temperature," *Int. J. Sci. Technol. Res.*, vol. 9, no. 1, pp. 2763–2767, 2020.
- [22] A. Khusnani, "synthesis of thin films Cu / Ni by the electroplating method assisted by magnetic fields in magnetic field variations," Thesis. Indonesia: Ahmad Dahlan University, 2019.
- [23] I. Buriak, R. A. Fleck, A. Goltsev, N. Shevchenko, M. Petrushko, and T. Yurchuk, "Translation of Cryobiological Techniques to Socially Economically Deprived Populations—Part 1: Cryogenic Preservation Strategies," *J. Med. Device.*, vol. 14, no. 1, pp. 1–14, 2020.
- [24] T. Chowdhury, "Study of Self-Heating Effects in GaN HEMTsle. Thesis, USA: Arizona State University, 2013.
- [25] M. Toifur, B. Haryadi, and W. Rahmadani, "Prototype of low temperature sensor based on coils-resistance temperature detector enhanced with three-wire configurations bridge," *Contemp. Eng. Sci.*, vol. 8, no. 29, pp. 1351–1359, 2015.
- [26] J. Fraden. Handbook of Modern sensors: 4 th edition. New York: Springer, 2010.

- [27] A. Khusnani, M. Toifur, G. Maruto, and Y. Pramudya, "The effect of the magnetic field to microstructure and sensitivity of Cu/Ni film," *Univers. J. Electr. Electron. Eng.*, vol. 6, no. 5, pp. 84–89, 2019.
- [28] M. Toifur, J. Saputra, Okimustava, and A. Khusnani, "The effect of magnetic field on the performance of Cu/Ni as low-temperature sensor," *Int. J. Sci. Technol. Res.*, vol. 9, no. 1, pp. 3526–3532, 2020.
- [29] A. Ferreira, N. Martin, S. Lanceros-Méndez, and F. Vaz, "Tuning electrical resistivity anisotropy of ZnO thin films for resistive sensor applications," *Thin Solid Films*, vol. 654, no. 2017, pp. 93–99, 2018.
- [30] S. Bigham, A. Fazeli, and S. Moghaddam, "Physics of microstructures enhancement of thin film evaporation heat transfer in microchannels flow boiling," *Sci. Reports, Dep. Mech. Aerosp. Eng. Univ. Florida, Gainesville, FL 32611, USA*, vol. 7, no. 44745, pp. 1–11, 2017.
- [31] B. Li, M. H. Parekh, R. A. Adams, T. E. Adams, C. T. Love, V. G. Pol, and V. Tomar, "Lithium-ion Battery Thermal Safety by Early Internal Detection, Prediction and Prevention," *Sci. Reports* 9, vol. 9, no. 13255, pp. 1–11, 2019.
- [32] F. Yang, G. Li, J. Yang, Z. Wang, D. Han, F. Zheng, and S. Xu, "Measurement of local temperature increments induced by cultured HepG2 cells with micro-thermocouples in a thermally stabilized system," *Sci. Rep.*, vol. 7, no. 1, pp. 1–12, 2017.
- [33] M. Toifur, Y. Yningsih, and A. Khusnani, "Microstructure, thickness and sheet resistivity of Cu / Ni thin film produced by electroplating technique on the variation of electrolyte temperature," *J. Phys. Conf. Ser.*, no. (012053), pp. 1–10, 2018.
- [34] M. Toifur, M. L. Khansa, Okimustava, A. Khusnani, and Ridwan, "The Effect of Deposition Time on the Voltage Range and Sensitivity of Cu/Ni as Low-Temperature Sensor Resulted from Electroplating Assisted by a Transverse Magnetic Field," *Key Eng. Mater.*, vol. 855, pp. 185–190, 2020.
- [35] S. N. D. Layers, X. Cao, T. Wang, K. D. T. Ngo, S. Member, and G. Lu, "Characterization of Lead-Free Solder and Using Thermal Impedance," *IEEE Trans. Components, Packag. Manuf. Technol.*, vol. 1, no. 4, pp. 495–501, 2011.
- [36] P. Kassanos, S. Anastasova, and H. Yang, G, "Implantable sensors and systems: From theory to practice," in *Implantable Sensors and Systems: From Theory to Practice*, Springer International Publishing, 2018, pp. 1–646.
- [37] B. Davaji, H. D. Chou, M. Malakoution, J.K. Lee, G. Panin, T. W. Kang, and C. H. Lee, "A patterned single layer graphene resistance temperature sensor," *Sci. Rep.*, vol. 7, no. 8811, pp. 1–10, 2017.
- [38] C. Yan, J. Wang, and P. S. Lee, "Stretchable graphene thermistor with tunable thermal index," *ACS Nano*, vol. 9, no. 2, pp. 2130–2137, 2015.
- [39] L. Kang, Y. Shi, J. Zhang, J. Zhang, C. Huang, N. Zhang, Y. He, W. Li, C. Wang, X. Wu, and X. Zhou, "A flexible resistive temperature detector (RTD) based on in-situ growth of patterned Ag film on polyimide without lithography," *Microelectron. Eng.*, vol. 216, no. July, p. 111052, 2019.

# 15. 2020,M. Taufiqurrahman, Moh. Toifur, Ishafit, Okimustafa, Azmi Khusnani.pdf

---

## ORIGINALITY REPORT

---

8%

SIMILARITY INDEX

---

### PRIMARY SOURCES

---

1	<a href="http://eprints.undip.ac.id">eprints.undip.ac.id</a> Internet	73 words — 2%
2	<a href="http://elartu.tntu.edu.ua">elartu.tntu.edu.ua</a> Internet	19 words — 1%
3	<a href="http://ir.uitm.edu.my">ir.uitm.edu.my</a> Internet	15 words — < 1%
4	<a href="http://jurnal.ulb.ac.id">jurnal.ulb.ac.id</a> Internet	14 words — < 1%
5	<a href="http://pubs.rsc.org">pubs.rsc.org</a> Internet	14 words — < 1%
6	<a href="http://pure.manchester.ac.uk">pure.manchester.ac.uk</a> Internet	13 words — < 1%
7	Sanghun Jeon, Soo-Chul Lim, Tran Quang Trung, Minhyun Jung, Nae-Eung Lee. "Flexible Multimodal Sensors for Electronic Skin: Principle, Materials, Device, Array Architecture, and Data Acquisition Method", Proceedings of the IEEE, 2019 Crossref	12 words — < 1%
8	Chen, Gang, Lin Yu, Yun-Hui Mei, Xin Li, Xu Chen, and Guo-Quan Lu. "Reliability comparison between	9 words — < 1%

SAC305 joint and sintered nanosilver joint at high temperatures for power electronic packaging", Journal of Materials Processing Technology, 2014.

Crossref

---

9	<a href="https://docplayer.cz">docplayer.cz</a> Internet	9 words — < 1%
10	<a href="https://www.oulu.fi">www.oulu.fi</a> Internet	9 words — < 1%
11	Muh. Hajar Akbar, Sunardi -, Imam Riadi. "Analysis of Steganographic on Digital Evidence using General Computer Forensic Investigation Model Framework", International Journal of Advanced Computer Science and Applications, 2020 Crossref	8 words — < 1%
12	<a href="https://arts.units.it">arts.units.it</a> Internet	8 words — < 1%
13	<a href="https://dokumen.pub">dokumen.pub</a> Internet	8 words — < 1%
14	<a href="https://repositorium.uminho.pt">repositorium.uminho.pt</a> Internet	8 words — < 1%
15	<a href="https://repository.kaust.edu.sa">repository.kaust.edu.sa</a> Internet	8 words — < 1%
16	<a href="https://research.library.mun.ca">research.library.mun.ca</a> Internet	8 words — < 1%
17	<a href="https://tel.archives-ouvertes.fr">tel.archives-ouvertes.fr</a> Internet	8 words — < 1%
18	<a href="https://www.favorit-ec.ru">www.favorit-ec.ru</a> Internet	

---

8 words — < 1%

---

19 [www.iscientific.org](http://www.iscientific.org)  
Internet

8 words — < 1%

---

20 Vania Rahmawaty, Endah Kinarya Palupi,  
Nazopatul Patonah, Tony Sumaryada, Irzaman.  
"The Mole Fraction Effect on Magnetic Properties of  
 $\text{Ba}_x\text{Sr}_{1-x}\text{TiO}_3$  ( $x = 0;$   
0.125; 0.25; 0.375; 0.500) Thin Film", Key Engineering Materials,  
2020  
Crossref

7 words — < 1%

---

EXCLUDE QUOTES OFF

EXCLUDE SOURCES OFF

EXCLUDE BIBLIOGRAPHY ON

EXCLUDE MATCHES OFF